DOI: 10.1002/cmdc.201402272

# Non-natural Acetogenin Analogues as Potent *Trypanosoma brucei* Inhibitors

Gordon J. Florence,* Andrew L. Fraser, Eoin R. Gould, Elizabeth F. B. King, Stefanie K. Menzies, Joanne C. Morris, Lindsay B. Tulloch, and Terry K. Smith*[a]

Neglected tropical diseases remain a serious global health concern. Here, a series of novel bis-tetrahydropyran 1,4-triazole analogues based on the framework of chamuvarinin, a polyketide natural product isolated from the *annonaceae* plant species are detailed. The analogues synthesized display low micromolar trypanocidal activities towards both bloodstream and insect forms of *Trypanosoma brucei*, the causative agent of African sleeping sickness, also known as Human African Trypanosomiasis (HAT). A divergent synthetic strategy was adopted for the synthesis of the key tetrahydropyran intermediates to enable rapid access to diastereochemical variation either side of the 1,4-triazole core. The resulting diastereomeric analogues displayed varying degrees of trypanocidal activity and selectivity in structure–activity relationship studies. Together, the biological potency and calculated lipophilicity values indicate that while there is room for improvement, these derivatives may represent a promising novel class of anti-HAT agents.

## Introduction

Neglected tropical diseases are a continuing health concern in developing countries due to the lack of effective prevention methods and therapeutic agents.[1] One of these prevalent neglected tropical diseases, which has been slowly attracting attention over the past few years, is African sleeping sickness or Human African Trypanosomiasis (HAT), caused by the protozoan parasite *Trypanosoma brucei* that is transmitted by the bite of the Tsetse fly. HAT is a major health concern in sub-Saharan Africa threatening more than 60 million people. The annual mortality rate of HAT estimated by the World Health Organization (WHO) stands at approximately 8000 with less than 30 000 new cases per year based on recent reports.[2] At present, the treatment for HAT is extremely limited and dependent upon the disease stage of HAT infection—the lymphatic first stage or the second neurological stage when the *T. brucei* parasite has crossed the blood–brain barrier. Four drugs are used in the treatment of HAT (Figure 1), namely suramin (**1**) and pentamidine (**2**) for stage 1 HAT, and melarsoprol (**3**) and eflornithine (**4**) for stage 2.

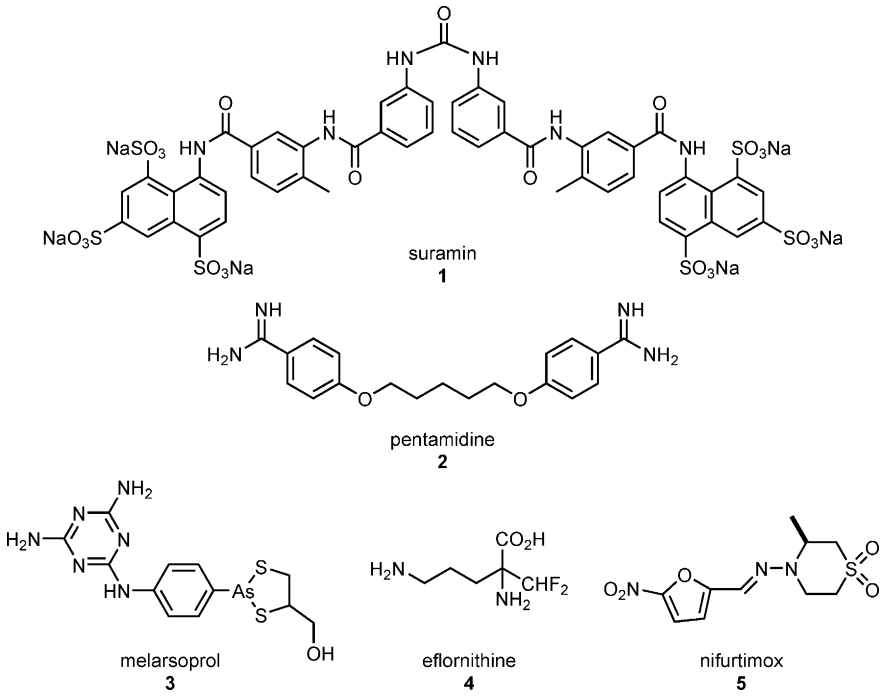


**Figure 1.** Current drugs for treatment of Human African trypanosomiasis (HAT).

These drugs are difficult to administer to patients, often requiring lengthy infusion rates; they have varying degrees of human toxicity and resistance is becoming a significant problem.[3] In an effort to decrease the costs associated with these

[a] *Dr. G. J. Florence, A. L. Fraser, Dr. E. R. Gould, E. F. B. King, S. K. Menzies, Dr. J. C. Morris, Dr. L. B. Tulloch, Prof. T. K. Smith*
*EaStCHEM School of Chemistry, Biomedical Sciences Research Complex*
*University of St Andrews, North Haugh, St Andrews, KY16 9ST (UK)*
*E-mail: gjf1@st-andrews.ac.uk*
*tks1@st-andrews.ac.uk*

Supporting information for this article is available on the WWW under http://dx.doi.org/10.1002/cmdc.201402272.

  

drugs, improve the logistics of their administration, and combat drug resistance (a common problem associated with parasitic diseases), a nifurtimox–eflornithine combination therapy (NECT; nifurtimox **5** is used clinically to treat Chagas disease) has been recently introduced for stage 2 HAT by the WHO.[4] This combination therapy maintains the efficacy of eflornithine at lower dosages, while decreasing the toxic side effects associated with eflornithine monotherapy. Despite the success of NECT, there is a lack of new effective therapeutic agents, and the onset drug resistance remains a serious threat to current therapies,[5] highlighting the urgent demand for the development of new drug-like molecules and their clinical implementation as effective HAT therapies.

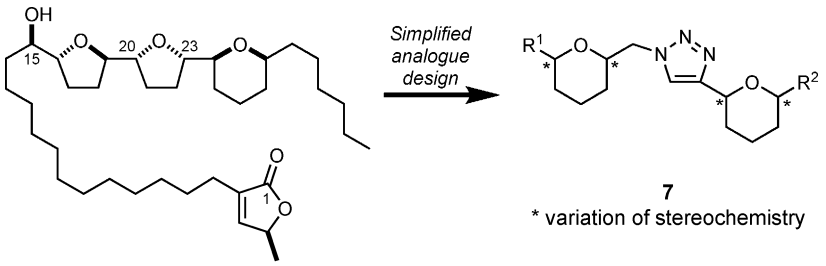


**Figure 2.** Rationale for simplified analogue design.

The acetogenins are a class of polyketide natural products isolated from the *annonaceae* plant species found in the tropical regions of West Africa and South America.[6,7] Chamuvarinin (**6**; Figure 2) was isolated in 2004 by Laurens et al. from the roots of the bush banana plant *Uvaria chamae* and showed significant cytotoxicity against the KB 3-1 cervix cancer cell line ($IC_{50}$ = 0.8 nM).[8] In 2011, we reported the total synthesis of chamuvarinin (**6**); we showed that **6** and a series of synthetic derivatives exhibited low micromolar activities towards both the blood-stream and procyclic forms of *T. brucei*.[9] These encouraging preliminary results and the limited investigations into trypanocidal activity of the acetogenins[10] prompted our initial interest in designing simplified analogues of **6**, which retain the important structural features of the acetogenin family of natural products. In an effort to decrease structural complexity, it was hypothesized that a 1,4-triazole motif could form an effective spatial mimic of the central C20–C23 tetrahydrofuran (THF) motif found in chamuvarinin (**6**). The synthesis

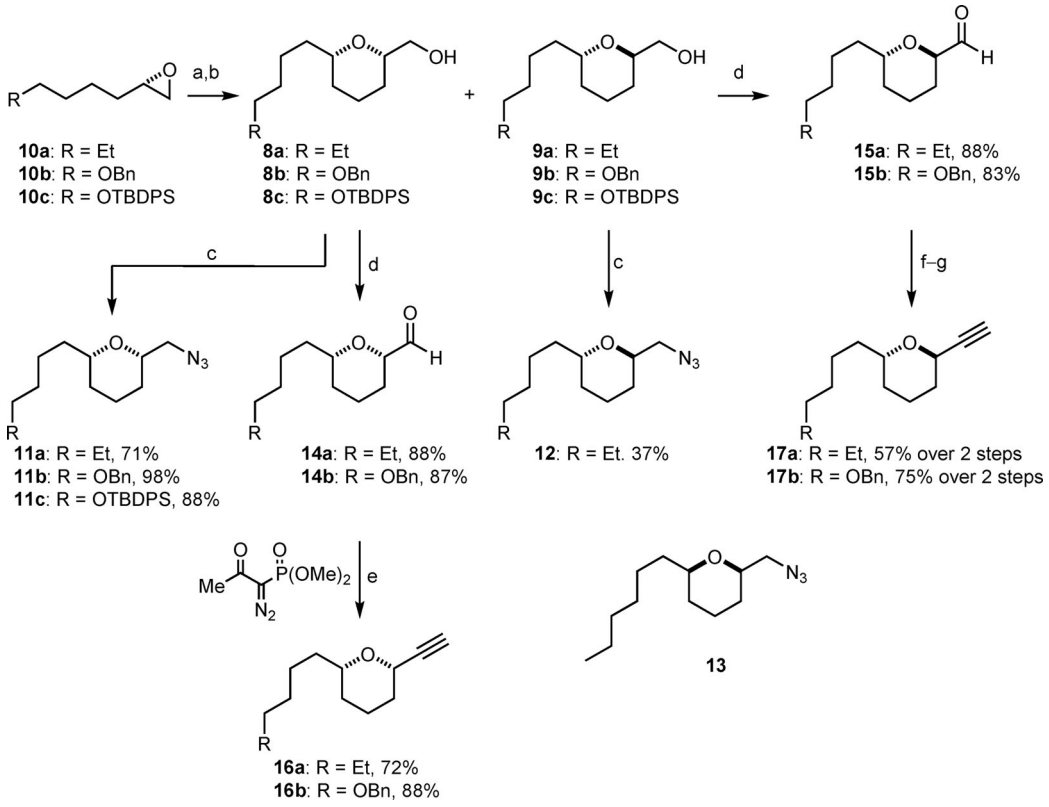


**Scheme 1.** Synthesis of azides **11a–c**, **12** and **13** and alkynes **16a–b** and **17a–b**. *Reagents and conditions*: a) $CH_2CHCH_2CH_2MgBr$, CuI, THF, −40 °C→RT, 2 h; b) *m*-CPBA, $CH_2Cl_2$, 0 °C→RT, 3 h; then (±)-CSA (20 mol%), RT, 2.5–18 h; c) $PPh_3$, *i*$Pr_2$NEt, DIAD, DPPA, 0 °C→RT, 16 h; d) $(COCl)_2$, DMSO, $CH_2Cl_2$, $Et_3N$, −78 °C→RT, 1 h; e) dimethyl diazo-2-oxopropylphosphonate, $K_2CO_3$, MeOH, RT, 16 h; f) $CBr_4$, $PPh_3$, $CH_2Cl_2$, −78 °C, 45 min; g) *n*BuLi, THF, −78 °C, 1.5 h. Abbreviations: (±)-camphorsulfonic acid [(±)-CSA]; 3-chloroperbenzoic acid (*m*-CPBA); diisopropyl azodicarboxylate (DIAD); dimethyl sulfoxide (DMSO); diphenyl phosphoryl azide (DPPA).

and incorporation of THF motifs are notoriously difficult, hence the C16–19 THF ring system of **6** was substituted with the readily accessible and manageable tetrahydropyran (THP) motif (**7** in Figure 2). The heterocyclic spacer was envisioned to arise from the "click" reaction of two THP subunits, whilst the butenolide moiety could be appended to the ether core in an analogous manner to **6** by a suitable length alkyl spacer.

## Results and Discussion

### Chemistry

As outlined in Scheme 1, intermediate THP alcohols **8a** and **9a** could be readily assembled in three steps from (*S*)-epoxyoctane (**10a**)[11] via copper(I)-promoted ring opening of **10a** with homoallyl magnesium bromide followed by 3-chloroperbenzoic acid (*m*-CPBA) epoxidation and subsequent in situ acid-mediated ring closure to provide a readily separable mixture of diastereomeric alcohols **8a** and **9a**. This divergent approach provided an excellent opportunity to introduce structural variation within the THP scaffolds. With the alcohols in hand, both diastereomers could be independently converted to the azide by Mitsunobu reaction (diphenylphosphoryl azide (DPPA), diisopropyl azodicarboxylate (DIAD), *N*,*N*-diisopropylethylamine, triphenylphosphine) of alcohols **8a** and **9a** to give **11a** and **12**.[12] The enantiomeric *syn* azide (**13**) could be accessed in an analogous manner from (*R*)-epoxyoctane.[11] For the alkyne subunits, *syn*-**8a** and *anti*-**9a** alcohols were oxidized under Swern conditions to afford aldehydes **14a** and **15a** in excellent yields, and subsequent exposure of **14a** to Ohira–Bestmann homologation[13] gave exclusively *syn*-**16a** in 72% yield. Due to epimerization of aldehyde **15a** under the mildly basic condi-

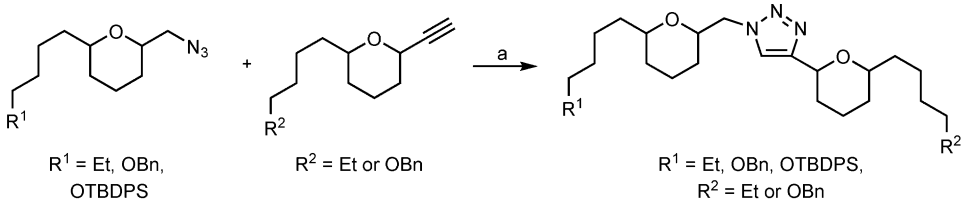


| Entry | Azide | Alkyne | Product | Yield [%] |
|---|---|---|---|---|
| 1 | **11a**: $R^1$ = Et | **16a**: $R^2$ = Et | **18a**: $R^1$ = Et, $R^2$ = Et | 71 |
| 2 | **11a**: $R^1$ = Et | **16b**: $R^2$ = OBn | **18b**: $R^1$ = Et, $R^2$ = OBn | 70 |
| 3 | **11b**: $R^1$ = OBn | **16a**: $R^2$ = Et | **18c**: $R^1$ = OBn, $R^2$ = Et | 41 |
| 4 | **11c**: $R^1$ = OTBDPS | **16b**: $R^2$ = OBn | **18d**: $R^1$ = OTBDPS, $R^2$ = OBn | 68 |
| 5 | **11a**: $R^1$ = Et | **17a**: $R^2$ = Et | **19a**: $R^1$ = Et, $R^2$ = Et | 75 |
| 6 | **11a**: $R^1$ = Et | **17b**: $R^2$ = OBn | **19b**: $R^1$ = Et, $R^2$ = OBn | 65 |
| 7 | **12**: $R^1$ = Et | **17a**: $R^2$ = Et | **20a**: $R^1$ = Et, $R^2$ = Et | 51 |
| 8 | **12**: $R^1$ = Et | **17b**: $R^2$ = OBn | **20b**: $R^1$ = Et, $R^2$ = OBn | 77 |
| 9 | **12**: $R^1$ = Et | **16a**: $R^2$ = Et | **21a**: $R^1$ = Et, $R^2$ = Et | 35 |
| 10 | **12**: $R^1$ = Et | **16b**: $R^2$ = OBn | **21b**: $R^1$ = Et, $R^2$ = OBn | 76 |
| 11 | **13**: $R^1$ = Et | **16b**: $R^2$ = OBn | **22**: $R^1$ = Et, $R^2$ = OBn | 43 |

**Scheme 2.** Synthesis of triazole analogues **18a–d**, **19a,b**, **20a,b**, **21a,b** and **22**. *Reagents and conditions*: a) $CuSO_4 \cdot 5H_2O$, Na ascorbate, $H_2O$, *t*BuOH, RT, 16 h.

tions, an alternative two-step Corey–Fuchs homologation[14] approach was adopted, giving **17a** in 70% yield. The incorporation of terminal oxygenation as a functional handle for extended elaboration was achieved by synthesis of the corresponding benzylated and silylated series of azides **11b**,**c** and alkynes **16b** and **17b** from epoxides **10b** and **10c**.

The central 1,4-triazole scaffold was conveniently installed by application of the copper(I)-catalyzed Huisgen 1,3-dipolar cycloaddition (Scheme 2).[15] Thus, diastereomeric analogues of the alkyl, benzylated and silylated bis-THP triazole motifs were synthesized by treatment of the corresponding azides **11a**–**c**, **12**, **13** and alkynes **16a**,**b**, **17a**,**b** under "click" reaction conditions (copper(II) sulfate, sodium ascorbate) to afford triazole products **18a**–**d**, **19a**,**b**, **20a**,**b**, **21a**,**b** and **22** in good yields.

Benzylated **18b-c**, **19b**, **20b**, **21b** and **22** analogues, outlined in Scheme 3, were deprotected under atmospheric hydrogenolysis (20% $Pd(OH)_2/C$, $H_2$) to the corresponding alcohols **23**–**28** (entries 1–6; Scheme 3) in excellent yields.

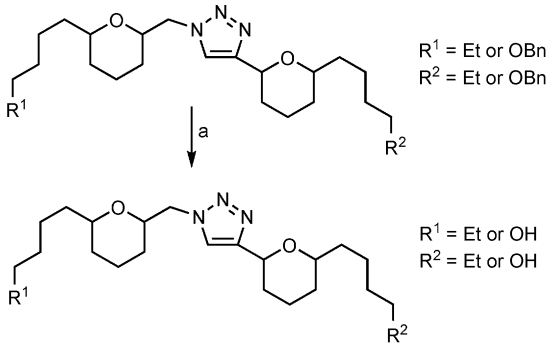


| Entry | Triazole | Product | Yield [%] |
|---|---|---|---|
| 1 | **18b**: $R^1$ = Et, $R^2$ = OBn | **23**: $R^1$ = Et, $R^2$ = OH | 92 |
| 2 | **19b**: $R^1$ = Et, $R^2$ = OBn | **24**: $R^1$ = Et, $R^2$ = OH | 95 |
| 3 | **20b**: $R^1$ = Et, $R^2$ = OBn | **25**: $R^1$ = Et, $R^2$ = OH | 93 |
| 4 | **21b**: $R^1$ = Et, $R^2$ = OBn | **26**: $R^1$ = Et, $R^2$ = OH | 92 |
| 5 | **22**: $R^1$ = Et, $R^2$ = OBn | **27**: $R^1$ = Et, $R^2$ =OH | 90 |
| 6 | **18c**: $R^1$ = OBn, $R^2$ = Et | **28**: $R^1$ = OH, $R^2$ = Et | 100 |

**Scheme 3.** Synthesis of alcohols **23**–**28**. *Reagents and conditions*: a) 20% $Pd(OH)_2/C$, $H_2$ (1 atm), EtOH, RT, 1.5 h.

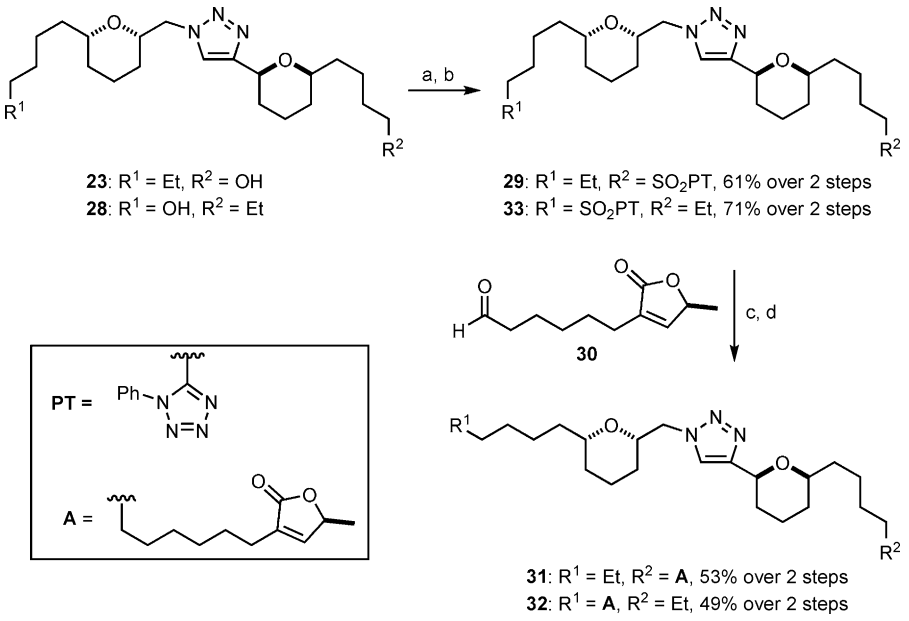


**Scheme 4.** Synthesis of triazoles **31** and **32**. *Reagents and conditions*: a) 1*H*-mercaptophenyltetrazole, $PPh_3$, DIAD, 0 °C, 3 h; b) $(NH_4)_6Mo_7O_{24}{\cdot}4H_2O$, $H_2O_2$, EtOH, 0 °C→RT, 16 h; c) NaHMDS, THF, −78 °C; then **30**, THF −78→−20 °C, 1.5 h; d) $TsNHNH_2$, NaOAc, DME, $H_2O$, 100 °C, 3 h. Abbreviations: diisopropyl azodicarboxylate (DIAD); dimethoxyethane (DME); sodium hexamethyldisilylazide (NaHMDS).

Having previously established structure–activity relationship (SAR) data for the advanced analogues of chamuvarinin, it was observed that incorporation of the butenolide side chain impacted positively on the trypanocidal activity. Thus, installation of the butenolide motif to successfully mimic chamuvarinin was accomplished in four steps from lead alcohol **23**, outlined in Scheme 4. Alcohol **23** was manipulated to sulfone **29** via a two-step Mitsunobu reaction and catalytic $Mo^{VI}$[7] oxidation protocol.[16] Subsequent Julia–Kocienski olefination[16] with aldehyde **30**[9,18] and diimide reduction[19] (*para*-toluenesulfonyl hydrazide, sodium acetate) provided advanced analogue **31**. To ascertain whether the triazole analogue would bind in a directional manner to the unknown protein target, analogue **32** was prepared in an analogous manner to **31** from alcohol **28** via sulfone **33**.

Having successfully installed the butenolide motif and in an effort to further extend the SAR data, bis-directional analogue **34**, outlined in Scheme 5, was synthesized in six steps from advanced triazole **18d**. Silyl deprotection of **18d** to alcohol **35**, followed by a Mitsunobu/oxidation protocol, gave sulfone **36**. Julia–Kocienski olefination of sulfone **36** with **30** and subsequent diimide reduction gave triazole **37**. Benzyl deprotection of **37** with boron trichloride furnished alcohol **34** in 23% yield. Diol analogue **38** was accessed in excellent yield from alcohol **35** under atmospheric hydrogenolysis.

### Structure–activity relationship summary

The primary mode of action for acetogenins in mammalian cells is inhibition of complex I of the mitochondrial electron transport chain (ETC).[20] In contrast, bloodstream (BSF) *T. brucei* lacks functional complexes I, III and IV and instead relies on al-

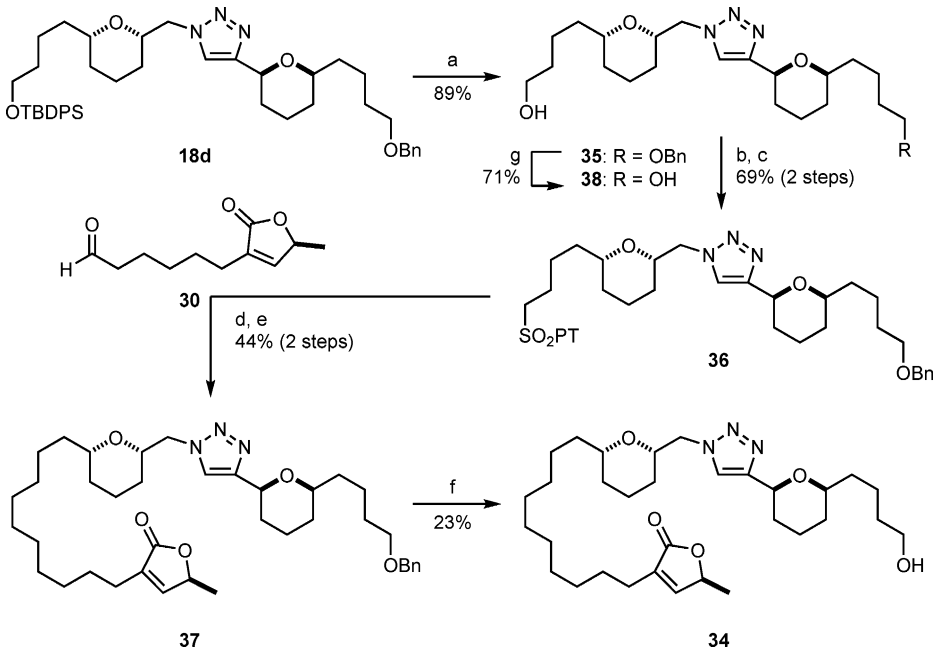


**Scheme 5.** Synthesis of advanced alcohol **34**. *Reagents and conditions*: a) TBAF, THF, 0 °C→RT, 4 h; b) 1*H*-mercaptophenyltetrazole, $PPh_3$, DIAD, 0 °C, 16 h; c) $(NH_4)_6Mo_7O_{24}{\cdot}4H_2O$, $H_2O_2$, EtOH, 0 °C→RT, 16 h; d) NaHMDS, THF, −78 °C; then **30**, THF −78→−20 °C, 3 h; e) $TsNHNH_2$, NaOAc, DME, $H_2O$, 100 °C, 3 h; f) $BCl_3{\cdot}SMe_2$, $CH_2Cl_2$, −78 °C→RT, 16 h; g) 20% $Pd(OH)_2/C$, $H_2$ (1 atm), EtOH, RT, 1.5 h. Abbreviations: diisopropyl azodicarboxylate (DIAD); dimethoxyethane (DME); sodium hexamethyldisilylazide (NaHMDS); tetrabutylammonium fluoride (TBAF).

ternative oxidases (TAO, AOX2) to enable mitochondrial respiration, while the procyclic (Pro) form expresses both a fully functional ETC and the alternative oxidases.[21] Thus in order to assess whether the triazole-based analogues share a common mitochondrial target and identify key structural features required for parasitic inhibition, screening against the BSF and Pro forms of *T. brucei* and the mammalian HeLa cell line[22] was performed (Table 1). From the data, it was evident that the stereochemistry surrounding the THP ring systems and the functionalization of the terminal motifs impacted on the *T. brucei* inhibition profile. In comparison to chamuvarinin (**6**), the initial set of diastereomeric alkyl triazoles **20a**, **21a** and **18a** (entries 1, 4, 7; Table 1) were more than 17 times less potent, indicating that stereochemistry has little effect on the inhibition profile. Surprisingly, analogue **19a** (entry 12; Table 1) displayed good levels of *T. brucei* inhibition with an $EC_{50}$ value of 7.6± 0.3 μM and moderate levels of parasite selectivity (SI = 21.9).

Introduction of terminal oxygenation as a handle for further manipulation to one side of the alkyl side chain, analogues **21b**, **18b**, **19b** and **22** (entries 5, 8, 13, 15; Table 1), resulted in good micromolar activities with $EC_{50}$ values below 10 μM. Interestingly, the *anti–anti* analogue **20b** (entry 2; Table 1) was devoid of HeLa and *T. brucei* activity. By comparison, analogue **21b** (entry 5; Table 1) displayed good levels of parasite inhibition and selectivity, with a selectivity index (SI) value of 23. For analogues **24** and **27** (entries 14 and 16; Table 1), removal of the benzyl group resulted in approximately twofold loss in parasite activity. Removal of the benzyl group from analogue **21b** (entry 5; Table 1) to give **26** (entry 6; Table 1) led to a significant loss in parasitic activity and selectivity: $EC_{50}$ values of 3.1 ± 0.1 and 72.4 ± 3.9 μM and SI values of 23 and 0.8, respectively. The *anti–anti* analogue (**25**; entry 3; Table 1) was still devoid of parasitic activity, despite transformation to the free hydroxy. Gratifyingly, introducing the free hydroxy to analogue **23** (entry 9; Table 1) led to a slight increase in *T. brucei* inhibition, and **23** has shown comparable levels of parasitic activity to that of chamuvarinin (**6**): $EC_{50}$ values of 1.80 ± 0.10 and 1.4 ± 0.1 μM, respectively.

On the basis of **23**, bis-directional analogue **35** (entry 10; Table 1) was tested in the hope of further improving the activity. Unfortunately, **35** was nine times less potent than **23**, and subsequent removal of the benzyl group to give diol **38** (entry 11; Table 1) resulted in significantly diminished activities. Comparison of the biological data for the ethyl, benzyl and alcohol triazole series implies that the benzyl group may be potentially interacting with residues at a protein target site, which an alcohol group cannot accommodate. Alternatively, or as well, the benzyl group may be able to readily insert itself into the lipophilic membrane, whereas the hydrophilic alcohol incurs a greater penalty for membrane insertion.

The synthesis of triazole analogues with terminal oxygenation has provided a functional handle for further elaboration (Table 2). The non-natural chamuvarinin-like analogues previously reported revealed that introduction of the butenolide side chain resulted in a greater than fivefold increase in *T. brucei* activity. Encouraged by the potent activity of lead alcohol **23** (entry 1; Table 2), it was decided to incorporate the butenolide moiety based on this structure. Analogues **31** and **32** (entries 2 and 3; Table 2) clearly highlight the importance of the spatial orientation of the pendent butenolide side chain. While **31** was essentially inactive, **32** displayed low micromolar selective activities against both BSF and Pro forms of *T. brucei*, with $EC_{50}$ values of 3.2 ± 0.1 and 5.7 ± 0.6 μM, respectively and a selectivity index (BSF/HeLa) of 15.8. This suggests that although the structures are only subtly different at face value, their binding/interaction is highly specific and indicative of a protein target, rather than the biophysical properties of the compounds.

On the basis of the SAR data, incorporation of both the butenolide moiety and a benzyl-protected alcohol in place of the alkyl side chain indicated that benzyl analogue **37** (entry 4, Table 2) had similar activity to **32**. Removal of the benzyl group to reveal the free hydroxy analogue (**34**; entry 5, Table 2), was found to diminish activity and was nine-times less active than

**Table 1.** Structure–activity relationship (SAR) data for ethyl analogues **20a**, **21a**, **18a**, **19a**, benzyl analogues **20b**, **21b**, **18b**, **35**, **19b**, **22**, and alcohol analogues **23–27**, **38**.[a]

| Entry | Compound | | $EC_{50}$ [μM] BSF | Pro | HeLa | SI | Entry | Compound | | $EC_{50}$ [μM] BSF | Pro | HeLa | SI |
|---|---|---|---|---|---|---|---|---|---|---|---|---|---|
| 1 | 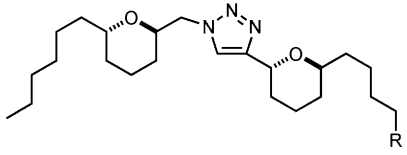 | **20a** R = Et | 24.6 ± 1.4 | 65.0 ± 3.1 | 33.0 ± 2.4 | 1.3 | 9 | 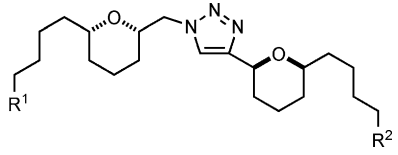 | **23** $R^1$ = Et $R^2$ = OH | 1.8 ± 0.1 | 0.8 ± 0.11 | 7.0 ± 1.0 | 3.9 |
| 2 | | **20b** R = OBn | 467.2 ± 40.3 | 236.6 ± 23.8 | > 1000 | > 2 | 10 | | **35** $R^1$ = OH $R^2$ = OBn | 16.2 ± 0.9 | 19.4 ± 0.5 | > 100 | > 6 |
| 3 | | **25** R = OH | 223.2 ± 21.8 | 87.9 ± 4.5 | 415.8 ± 35.3 | 1.9 | 11 | | **38** $R^1$ = $R^2$ = OH | 157.8 ± 13.2 | 99.0 ± 2.5 | > 250 | > 1.5 |
| 4 | 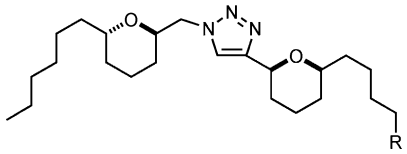 | **21a** R = Et | 37.2 ± 6.6 | 81.5 ± 4.5 | > 500 | > 6 | 12 | 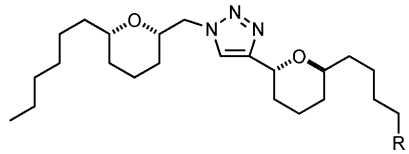 | **19a** R = Et | 7.6 ± 0.3 | 1.1 ± 0.1 | 166.6 ± 18.0 | 21.9 |
| 5 | | **21b** R = OBn | 3.1 ± 0.1 | 48.7 ± 3.6 | 71.4 ± 4.1 | 23 | 13 | | **19b** R = OBn | 10.1 ± 0.4 | 72.3 ± 5.3 | 76.0 ± 3.0 | 7.5 |
| 6 | | **26** R = OH | 72.4 ± 3.9 | 68.3 ± 7.2 | 59.7 ± 2.5 | 0.8 | 14 | | **24** R = OH | 17.5 ± 1.0 | 25.4 ± 1.3 | 26.9 ± 1.1 | 1.5 |
| 7 | 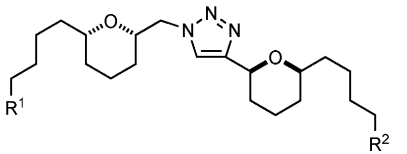 | **18a** $R^1$ = $R^2$ = Et | 48.7 ± 3.5 | 103.3 ± 3.5 | > 100 | > 2 | 15 | 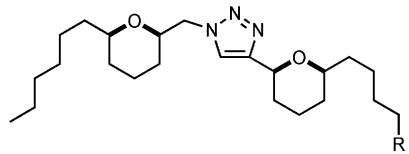 | **22** R = OBn | 8.2 ± 0.4 | 15.5 ± 1.0 | 37.5 ± 1.5 | 4.6 |
| 8 | | **18b** $R^1$ = Et $R^2$ = OBn | 8.7 ± 0.5 | 15.6 ± 0.3 | 45.5 ± 2.5 | 5.3 | 16 | | **27** R = OH | 19.2 ± 1.1 | 42.9 ± 2.4 | 101.0 ± 10.4 | 5.3 |

[a] $EC_{50}$ values were determined against bloodstream (BSF) and procyclic (Pro) *T. brucei*, or in mammalian HeLa cells. Data represent the mean ± SD of $n = 3$ independent experiments performed in triplicate. The selectivity index (SI) refers to BSF parasitic inhibition versus mammalian HeLa inhibition. For comparison: chamuvarinin (**6**): $EC_{50}$ = 1.4 ± 0.1 μM (BSF); 1.9 ± 0.1 μM (Pro); 2.9 ± 0.7 μM (HeLa); data taken from Ref. [9].

**Table 2.** Biological profiles for analogues **23**, **31**-**32**, **34** and **37**.

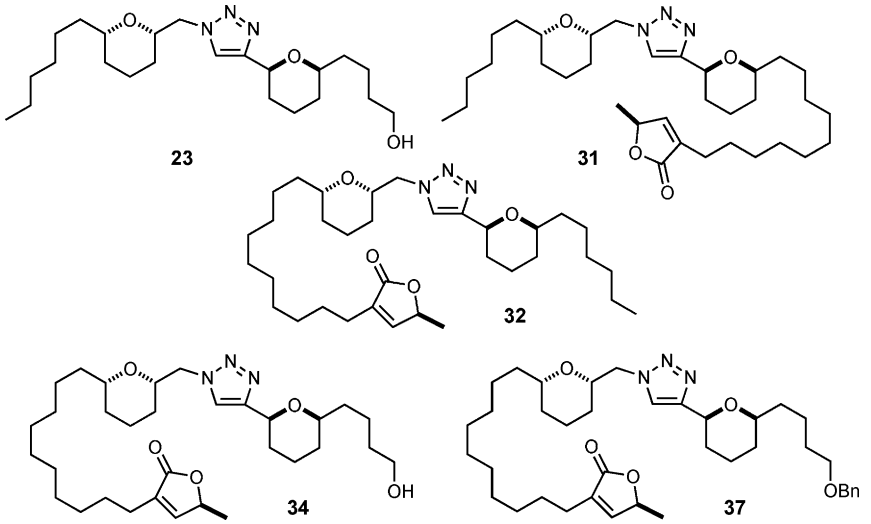


| Entry | Compd | $EC_{50}$ [μM] BSF | Pro | HeLa | SI |
|---|---|---|---|---|---|
| 1 | **23** | 1.8 ± 0.1 | 0.8 ± 0.1 | 7.0 ± 1.0 | 3.9 |
| 2 | **31** | > 500 | > 1000 | > 1000 | – |
| 3 | **32** | 3.2 ± 0.1 | 5.7 ± 0.6 | 50.8 ± 3.7 | 15.8 |
| 4 | **37** | 5.2 ± 0.3 | 19.2 ± 0.8 | 2.1 ± 0.4 | 0.4 |
| 5 | **34** | 28.5 ± 4.6 | 5.6 ± 0.6 | 8.3 ± 1.1 | 0.3 |

[a] $EC_{50}$ values were determined against bloodstream (BSF) and procyclic (Pro) *T. brucei*, or in mammalian HeLa cells. Data represent the mean ± SD of $n = 3$ independent experiments performed in triplicate. The selectivity index (SI) refers to BSF parasitic inhibition versus mammalian HeLa inhibition.

**32**, with $EC_{50}$ values of 28.5 ± 4.6 and 3.2 ± 0.1 μM, respectively. This may indicate that a non-hydrophilic arm on the opposite side of the butenolide moiety is required for maximum protein/analogue/lipid interaction.

### Lipophilic efficiency

A theoretical comparison of the triazole analogues molecular properties was conducted in an effort to highlight the lipophilicity of these compounds and provide an indication as to whether they would be suitable drug candidates. As outlined in Table 3, lead compound alcohol **23** (entry 1) possesses a suitable calculated lipophilicity (clog*P*) value of 5.163, has a molecular weight of less than 500, and has a suitable number of hydrogen-bond donors and acceptors, adhering to Lipinski's rule of five. Introduction of the butenolide moiety on one end of the THP ring system and an alkyl side chain on the opposite side in analogue **32** (entry 2, Table 3), led to an increased clog *P* value of 9. Exchange of the hydrophobic alkyl side chain with either a benzyl group (**37**; entry 4, Table 3) or a free hydroxy group (**34**; entry 3, Table 3) decreased the clog *P* values while increasing the potential for hydrogen-bond donation. Chamuvarinin itself (**6**; entry 5, Table 3) is calculated to have a high clog *P* value of 9, in line with the observed ability of acetogenin family members to cross the blood–brain barrier[23]

The lipophilic efficiency (Lip*E*) is a combination of the calculated lipophilicity (clog*P*) and the potency ($pEC_{50}$) of analogues to estimate the drug-likeness (Lip*E* > 5) of a compound. The calculated Lip*E* values for triazoles **23**, **32**, **34**, **37** and chamuvarinin **6** fall in the range +0.6 to −3.7 (Table 3), which although below the optimal value are in line with values often displayed by natural products and their derivatives.[24] Furthermore the Lip*E* values of our designed triazole analogues are comparable with bioactive compounds that cross the blood–brain barrier,[23,24] which when coupled with their toxicity towards *T. brucei*, provides the exciting prospect of developing an effective dual pronged treatment for both stage 1 and 2 HAT if selectivity profiles can be further improved.

### Molecular modelling

Our initial rationale for the design and synthesis of simplified triazole analogues was based on the molecular modelling of the central tricyclic core of chamuvarinin (**6**), as outlined in Figure 3 a, indicating that **6** adopts a "U-shape" conformation.[25] We hypothesized that a five-membered heterocyclic spacer (Figure 3 b,c) would act as an effective spatial mimic for the central THF core of **6** and thus retain potent biological activity. Modelling highlights that the lowest energy conformation of the *syn-syn* bis-THP rings is predicted to act as a better mimic of this "U-shaped" conformation than the corresponding *anti-anti*, and this would appear to be broadly borne out by the biological results.[25] The encouraging trypanocidal activity of the triazole com-

**Table 3.** Theoretical data of molecular properties for triazole analogues **6**, **23**, **32**, **34** and **37**.[a]

| Entry | Compd | $EC_{50}$ [μM] | $pEC_{50}$ | clog *P* | Lip *E* | MW | H bond donors | H bond acceptors |
|---|---|---|---|---|---|---|---|---|
| 1 | **23** | 1.8 ± 0.1 | 5.75 | 5.163 | 0.59 | 407.6 | 1 | 6 |
| 2 | **32** | 3.2 ± 0.1 | 5.49 | 9.056 | −3.57 | 571.8 | 0 | 7 |
| 3 | **34** | 28.5 ± 4.6 | 4.55 | 7.336 | −2.79 | 559.8 | 1 | 8 |
| 4 | **37** | 5.2 ± 0.3 | 5.29 | 8.935 | −3.65 | 649.9 | 1 | 8 |
| 5 | **6** | 1.4 ± 0.1 | 5.86 | 9.208 | −3.35 | 604.9 | 1 | 6 |

[a] $EC_{50}$ values were determined against bloodstream (BSF) *T. brucei*; data represent the mean ± SD of $n = 3$ independent experiments performed in triplicate. Theoretical molecular properties: (clog *P*); (Lip *E*); molecular weight (MW); number of H bond donors and acceptors, were calculated using Molinspiration Cheminformatics calculation of molecular properties and bioactivity scores (http://www.molinspiration.com/cgi-bin/properties).

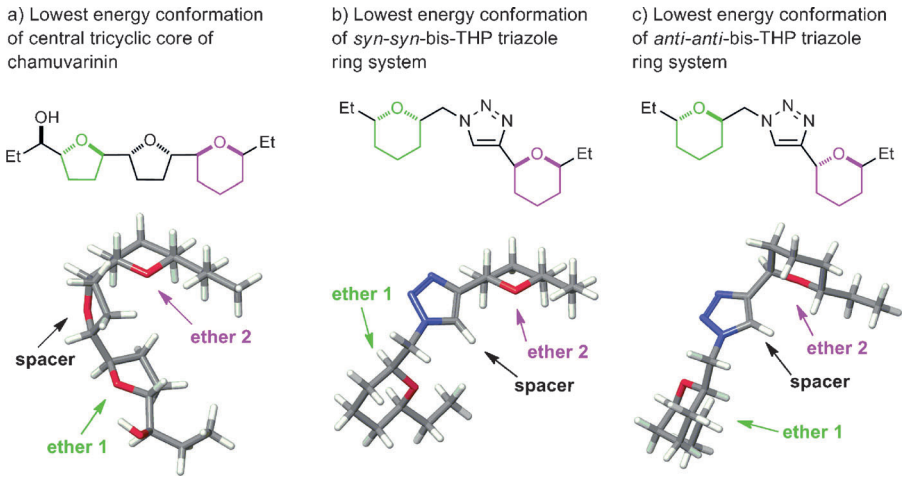


**Figure 3.** Molecular modelling of the lowest energy conformations for a) chamuvarinin framework; b) *syn-syn* triazole core; and c) *anti-anti* triazole core.

pounds discussed in this paper has now formed the basis of further design iterations and lead structure optimization. The evolving structure–activity relationships will be enabled by further cycles of iterative design towards the development of more potent and selective trypanocidal compounds.

## Conclusions

A focused library of 1,4-triazole-based acetogenin analogues was synthesized, and these analogues demonstrated low micromolar trypanocidal activities against both bloodstream and procyclic forms of *T. brucei*. Analogue **23** displayed comparable levels of *T. brucei* inhibition to that of natural product chamuvarinin (**6**), with $EC_{50}$ values of $1.8 \pm 0.1$ and $1.4 \pm 0.1$ μM, respectively, demonstrating that this series of triazole analogues are potential lead compounds for the development of an effective therapeutic agent for HAT. The acetogenins have long been established as mitochondrial Complex I inhibitors within mammalian cells, therefore, it is postulated that the analogues are targeting a protein within the mitochondrion of the parasite. The specific protein target and mode of action for parasite inhibition is currently undetermined for these analogues. However, analogues **31** and **32** clearly highlight that spatial orientation of the butenolide side chain impacts heavily on *T. brucei* inhibition. Current focus is to establish whether the analogues are disrupting mitochondrial functions, through the incorporation of fluorescent and affinity tags to lead triazole compounds in order to isolate specific proteins of interest, allowing them to be genetically and chemically validated.

## Experimental Section

For full experimental details, see the Supporting Information, available via http://dx.doi.org/10.1002/cmdc.201402272.

## Acknowledgements

*This work was funded by The Royal Society (UK), the Leverhulme Trust (UK), the UK Engineering and Physical Sciences Research Council (EPSRC) (G.J.F.) and the Wellcome Trust (UK) (T.K.S., WT 093228). The authors thank the EPSRC National Mass Spectrometry Service Centre (Swansea, UK) for mass spectrometry services.*

**Keywords:** acetogenin · Human African Trypanosomiasis (HAT) · neglected diseases · natural product analogues · stereochemistry · *Trypanosoma brucei*

[1] L. Zhou, G. Stewart, E. Rideau, N. J. Westwood, T. K. Smith, *J. Med. Chem.* **2013**, *56*, 796–806.
[2] *Trypanosomiasis, African*; World Health Organization (WHO), Geneva, Switzerland, **2012**; http://www.who.int/topics/trypanosomiasis_african/en/ (Accessed 19 June, **2014**).
[3] a) D. Steverding, *Parasites Vectors* **2010**, *3*, 15; b) V. Delespaux, H. P. de Koning, *Drug Resist. Updates* **2007**, *10*, 30–50.
[4] G. Priotto, S. Kasparian, W. Mutombo, D. Ngouama, S. Ghorashian, U. Arnold, S. Ghabri, E. Baudin, V. Buard, S. Kazadi-Kyanza, M. Ilunga, W. Mutangala, G. Pohlig, C. Schmid, U. Karunakara, E. Torreele, V. Kande, *Lancet* **2009**, *374*, 56–64.
[5] A. Y. Sokolova, S. Wyllie, S. Patterson, S. L. Ozam, K. D. Read, A. H. Fairlamb, *Antimicrob. Agents Chemother.* **2010**, *54*, 2893–2900.
[6] a) F. Q. Alali, X. X. Liu, J. L. McLaughlin, *J. Nat. Prod.* **1999**, *62*, 504–540; b) M. C. Zafra-Polo, B. Figadère, T. Gallardo, J. R. Tormo, D. Cortes, *Phytochemistry* **1998**, *48*, 1087–1117; c) M. C. Zafra-Polo, M. C. González, E. Estornell, S. Sahpaz, D. Cortes, *Phytochemistry* **1996**, *42*, 253–271; d) L. Zeng, Q. Ye, N. H. Oberlies, G. Shi, Z. M. Gu, K. He, J. L. McLaughlin, *Nat. Prod. Rep.* **1996**, *13*, 275–306; e) J. K. Rupprecht, Y. H. Hui, J. L. McLaughlin, *J. Nat. Prod.* **1990**, *53*, 237–278.
[7] A. Bermejo, B. Figadère, M. C. Zafra-Polo, I. Barrachina, E. Estornell, D. Cortes, *Nat. Prod. Rep.* **2005**, *22*, 269–303.
[8] a) D. Fall, R. A. Duval, C. Gleye, A. Laurens, R. Hocquemiller, *J. Nat. Prod.* **2004**, *67*, 1041–1043; b) S. Derbré, E. Poupon, C. Gleye, R. Hocquemiller, *J. Nat. Prod.* **2007**, *70*, 300–303.
[9] a) G. J. Florence, J. C. Morris, R. G. Murray, R. R. Vanga, J. D. Osler, T. K. Smith, *Org. Lett.* **2011**, *13*, 514–517; b) G. J. Florence, J. C. Morris, R. G. Murray, R. R. Vanga, J. D. Osler, T. K. Smith, *Chem. Eur. J.* **2013**, *19*, 8309–8320.
[10] a) S. Sahpaz, C. Bories, P. M. Loiseau, D. Cortès, R. Hocquemiller, A. Laurens, A. Cavé, *Planta Med.* **1994**, *60*, 538–540; b) A. I. Waechter, G. Yaluff, A. Inchausti, A. R. de Arias, R. Hocquemiller, A. Cavé, A. Fournet, *Phytother. Res.* **1998**, *12*, 541–544; c) S. Hoet, F. Opperdoes, R. Brun, J. Quetin-Leclercq, *Nat. Prod. Rep.* **2004**, *21*, 353–364.
[11] a) G. C. Paddon-Jones, C. S. P. McErlean, P. Hayes, C. J. Moore, W. A. Konig, W. Kitching, *J. Org. Chem.* **2001**, *66*, 7487–7495; b) S. E. Schaus, A. D. Brandes, J. F. Larrow, M. Tokunga, K. B. Hansen, A. E. Gould, M. E. Furrow, E. N. Jacobsen, *J. Am. Chem. Soc.* **2002**, *124*, 1307–1315.
[12] J. P. Scott, M. Alam, N. Bremeyer, A. Goodyear, T. Lam, R. D. Wilson, G. Zhou, *Org. Process Res. Dev.* **2011**, *15*, 1116–1123.
[13] a) S. Müller, B. Liepold, G. J. Roth, H. J. Bestmann, *Synlett* **1996**, 521–522; b) G. J. Roth, B. Liepold, S. G. Müller, H. J. Bestmann, *Synthesis* **2004**, 59–62.
[14] E. J. Corey, P. L. Fuchs, *Tetrahedron Lett.* **1972**, *13*, 3769–3772.

[15] a) V. V. Rostovtsev, L. G. Green, V. V. Fokin, K. B. Sharpless, *Angew. Chem.* **2002**, *114*, 2708 – 2711; *Angew. Chem. Int. Ed.* **2002**, *41*, 2596 – 2599; b) C. W. Tornøe, C. Christensen, M. Meldal, *J. Org. Chem.* **2002**, *67*, 3057 – 3064.
[16] H. S. Schultz, H. B. Freyermuth, S. R. Buc, *J. Org. Chem.* **1963**, *28*, 1140 – 1142.
[17] a) P. R. Blakemore, W. J. Cole, P. J. Kocieński, A. Morley, *Synlett* **1998**, 26 – 28; b) P. R. Blakemore, *J. Chem. Soc. Perkin Trans. 1* **2002**, 2563 – 2585; c) R. I. Dumeunier, I. E. Markó, *Modern Carbonyl Olefination: Methods and Applications* (Ed.: T. Takeda), Wiley-VCH, Weinheim, **2004**, pp. 104 – 150.
[18] Butenolide aldehyde **30** was synthesized in five steps from enantioenriched (*S*)-propylene oxide; see Ref. [8a].
[19] a) J. A. Marshall, M. Chen, *J. Org. Chem.* **1997**, *62*, 5996 – 6000; b) M. T. Crimmins, Y. Zhang, F. A. Diaz, *Org. Lett.* **2006**, *8*, 2369 – 2372.
[20] a) M. Degli Esposti, A. Ghelli, M. Ratta, D. Cortes, E. Estronell, *Biochem. J.* **1994**, *301*, 161 – 167; b) N. De Pedro, B. Cautain, A. Melguizo, F. Vicente, O. Genilloud, F. Pelaez, J. R. Tormo, *J. Bioenerg. Biomembr.* **2013**, *45*, 153 – 164.
[21] For a review, see: A. G. Tielens, J. J. van Hellemond, *Trends Parasitol.* **2009**, *25*, 482 – 490.
[22] Biological testing was performed using the Alamar Blue viability test as described in: J. Mikus, D. Steverding, *Parasitol. Int.* **2000**, *48*, 265 – 269.
[23] P. Champy, G. U. Höglinger, J. Féger, C. Gleye, R. Hocquemiller, A. Laurens, V. Guérineau, O. Laprévote, F. Medja, A. Lombès, P. P. Michel, A. Lannuzel, E. C. Hirsch, M. Ruberg, *J. Neurochem.* **2004**, *88*, 63 – 69.
[24] I. Jabeen, K. Pleban, U. Rinner, P. Chiba, G. F. Ecker, *J. Med. Chem.* **2012**, *55*, 3261 – 3273.
[25] Schrodinger Maestro (v9.7.014) and Macromodel (v10.4) were used for 10000 step Monte-Carlo searches using the MMFF force field.

Received: July 2, 2014
Published online on August 21, 2014